# Appendix

## 1 WRF SIMULATIONS

WRF simulations were performed from 2015-01-15 00:00:00 to 2016-01-14 23:00:00 local time in all the wind sites shown in Table S2. An example of the model domain used in the WRF simulations is depicted in Figure S1, for Olavarría wind site. Domains 1 and 2 are centered in the point of interest.

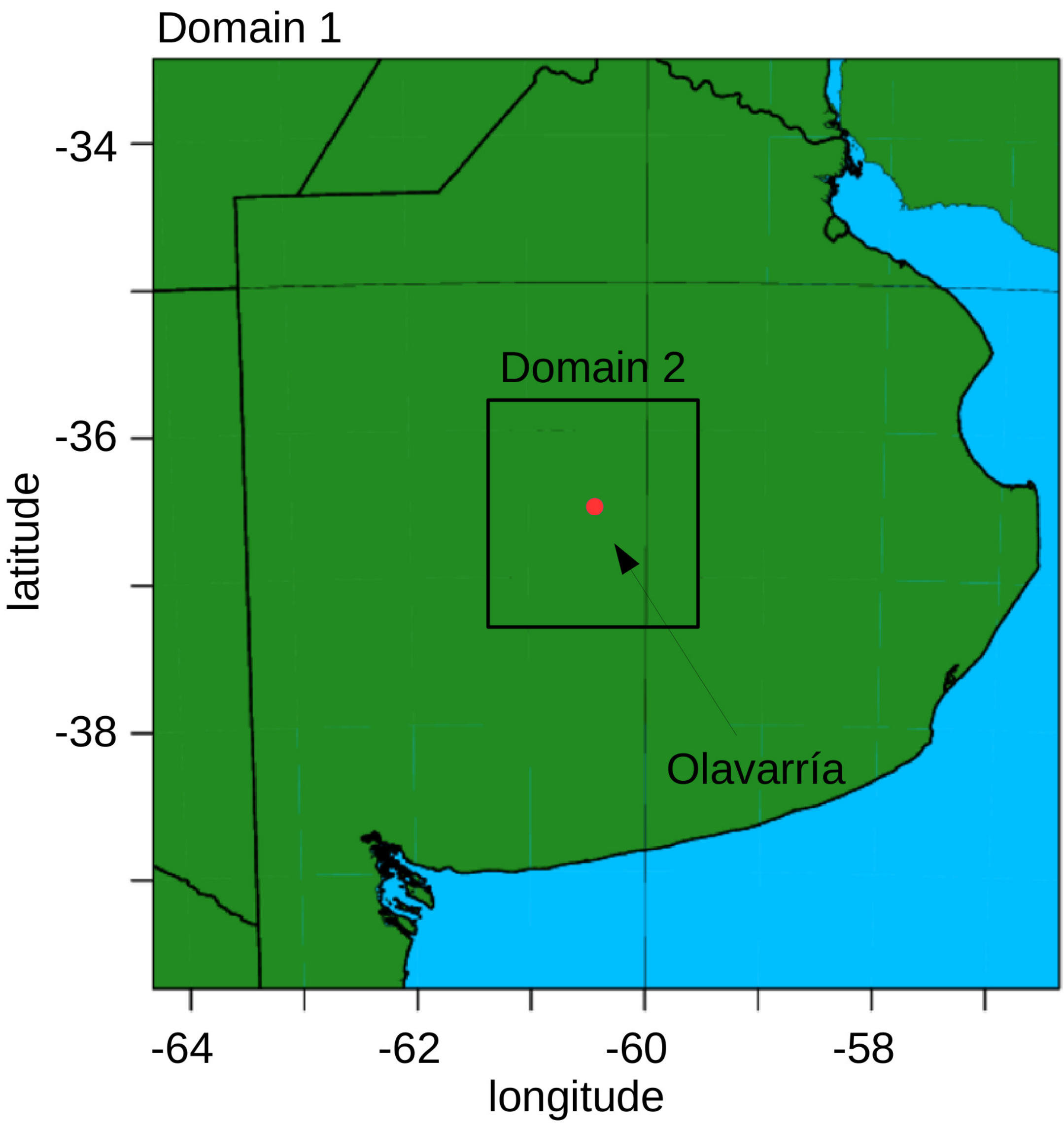


**Figure S1.** Example of domain used in WRF simulations, in this case for Olavarría (ID number 9). The box inside denotes the second domain with 3 times higher resolution.

MERRA2 wind data and WRF simulations are compared in Figure S2, which depicts hourly and monthly averages at all sites. Individual data can be seen in Table S2. In all cases the mean wind velocity simulated with WRF is higher. A noticeable example is Arauco, where mean velocity obtained with WRF almost doubles the value given by MERRA2. The topography at this location shows a great spatial variability, which is probably not represented by MERRA2 due to its coarse resolution ($> 50\,\mathrm{km}$)

Overall comparison shows that, besides obtaining higher wind speeds values with WRF, daily cycles are much more pronounced in WRF simulations. This can be seen when averaging daily and monthly cycles from all wind sites, as we show in Figure S2. Monthly cycles match between both data, although higher values are obtained with WRF. Instead, WRF express a much more defined daily cycle in all sites. This might be because of smaller scale effects which are not captured by MERRA. We will use WRF values for hourly calculation from now on.

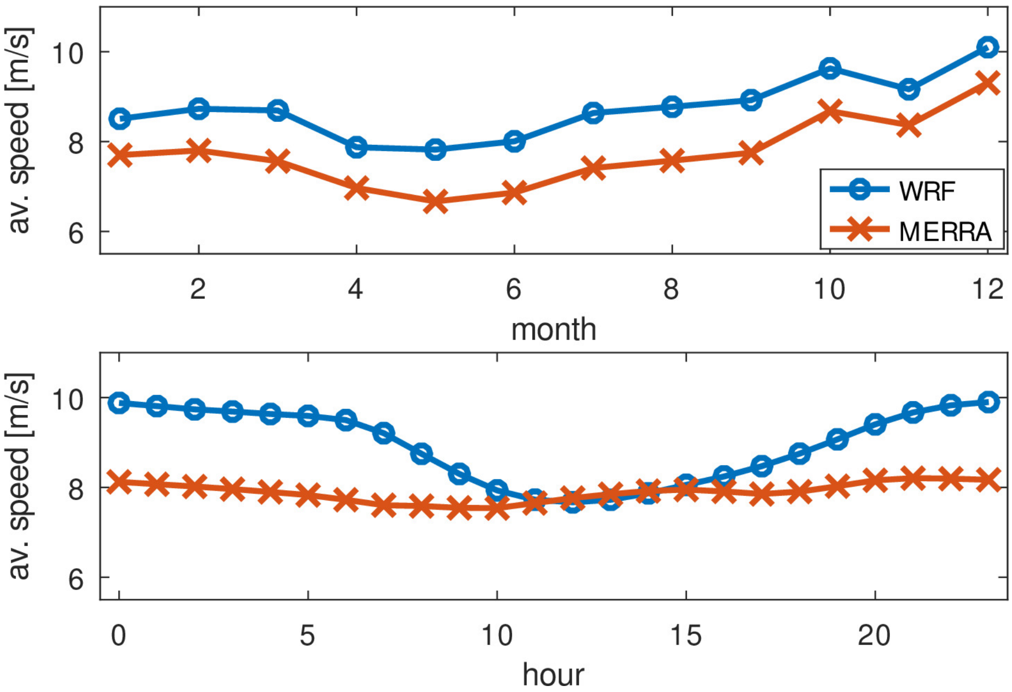


**Figure S2.** Daily (above) and monthly (below) cylcles from all wind sites computed with WRF and MERRA data.

We also computed the weibull $k$ factor for both MERRA2 and WRF hourly data, also shown in Table S2. WRF shows lower $k$ values, indicating a higher dispersion of velocity values.

## 2 CONVERSION OF WIND SPEED AND IRRADIANCE TO POWER

### 2.1 Wind speed to power

To convert wind speed time series to power we used a method based on the Wind Farm Virtual Model (Staffell and Green, 2014) (see Section **??** for detailed information about the scripts). We obtained wind speed data at 100 m height using WRF calculations at each site. We then choose between three $3.45\,\mathrm{MW}$ commercial wind generators power curves, depending on the mean wind speed of each site:

- Vestas V112 (class IEC IA - IB) for mean wind speeds close $10\,\mathrm{m\,s^{-1}}$
- Vestas V117 (class IEC IIA – IIB) for mean wind speeds close $8.5\,\mathrm{m\,s^{-1}}$
- Vestas V126 (class IIIA - IIIB) for mean wind speeds below $7.5\,\mathrm{m\,s^{-1}}$

The power curve was then smoothed using a gaussian filter to address the smoothing effect of having multiple turbines on each park. We then convolved wind speed values with the smoothed power curve.

By following this steps we are neglecting detailed information about the actual wind turbine generator to be installed at each site, plus the number of generators installed per park and its spatial configuration. We neither capture wake effects, which may have much more impact on the resulting power curve than power curve selection or smoothing filters. Such information is not on the scope of this study. In this work we only distinguish power classes following the first criteria described in the International Electrotechnical Commission international standard for wind turbine generators (IEC 61400). According to this norm (Commission et al., 2005), wind turbines classes are defined by 1) the average wind speed 2) the extreme 50-year gust and 3) the turbulence.

Table S2 shows the mean capacity factors obtained. We compared our results with data provided by the national grid administrator (Compañía Administradora del Mercado Mayorista Eléctrico de Argentina, CAMMESA) from 3 wind parks. Results are resumed in table S1. We found good agreement between combined WRF-VWF simulations and measured energy production.

## 2.2 Irradiance to power

For power production based on solar irradiance, we used the The Global Solar Energy Estimator (GSEE[1]), developed by Pfenninger and Staffel (Pfenninger and Staffell, 2016). This method calculates direct and diffuse irradiances via the BRL model (Ridley et al., 2010), using the short wave ground-level global irradiance variable SWGDN and top of atmosphere irradiance SWTDN from the closest MERRA2 grid point. Then, it uses the pyephem library (Rhodes, 2011) to compute the irradiance vector direction given time and location, and calculates the angle of incidence between irradiance and solar panels; whether panels are fixed or have tracking capabilities. Temperature data, which was also retrieved from MERRA, is used by the model to adjust the power output obtained through temperature-efficiency curves. Silicon panels are used for all parks.

Table S3 shows the mean capacity factors obtained. We compared our results with data provided by the national grid administrator (Compañía Administradora del Mercado Mayorista Eléctrico de Argentina, CAMMESA) from solar park Chimberas. Results are resumed in table S1. We found good agreement between GSEE model (feeded with MERRAII data) with measured energy production.

**Table S1.** Comparison of simulations and measured data at wind parks Arauco, Rawson and Loma Blanca (Trelew); and Chimberas solar park. WRF data compares better when there are local effects such as in Arauco wind park

| Park | Chimberas | Arauco | | Rawson | | Loma Blanca | |
|---|---|---|---|---|---|---|---|
| type | solar | wind | | wind | | wind | |
| period | 2015-2016 | 11/2015 | | 2015-2016 | | 2015-2016 | |
| data source | MERRA | WRF | MERRA | WRF | MERRA | WRF | MERRA |
| BIAS | +5% | -7% | -67% | +32% | +16% | +27% | +17% |
| hourl corr. | 0.69 | 0.64 | 0.43 | 0.65 | 0.69 | 0.72 | 0.70 |
| daily corr. | 0.94 | 0.79 | 0.26 | 0.87 | 0.88 | 0.88 | 0.86 |
| hourl RMSE | 50% | 65% | 67% | 72% | 67% | 64% | 63% |
| daily RMSE | 24% | 30% | 44% | 30% | 32% | 30% | 33% |

### Arauco wind park

We compared simulations with hourly production data from november 2015. Results are depicted in Figure S3 (A). Supposing an installed capacity of $27\,\mathrm{MW}$, the measured capacity factor is $0.44$. Using

[1] `https://github.com/renewables-ninja/gsee`

WRF and the VWF we obtained a slightly lower capacity factor of $0.41$. The correlation between data is $0.66$ and the root mean square error between measured and simulated power is $7.5\,\mathrm{MW}$, which is $\sim 65\%$ of the power average. We remark that using MERRA2 data the obtained capacity factor is $0.09$, clearly underestimating the site's capacity.

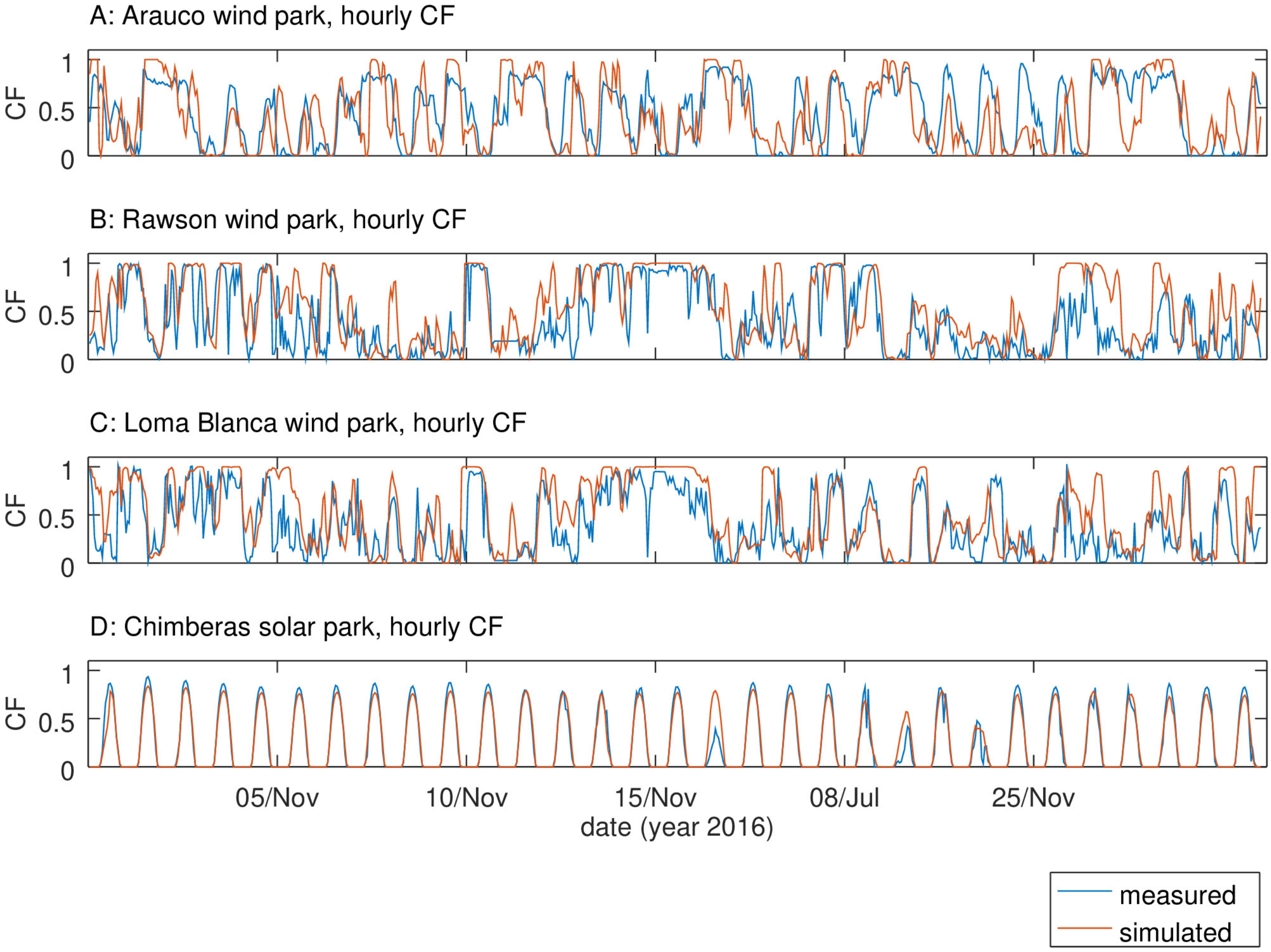


**Figure S3.** Comparison of hourly measured data from November 2016 with simulated power series. Simulations were obtained using the Virtual Wind Farm model (Staffell and Green, 2014; Staffell and Pfenninger, 2016) and WRF simulations for wind locations in panels (A), (B) and (C) and the The Global Solar Energy Estimator GSEE (Pfenninger and Staffell, 2016) using MERRA2 irradiance data for the solar location in panel (D).

## Loma Blanca and Rawson wind parks

We compared simulations with hourly production from Rawson and Loma Blanca wind parks, form the entire 2015-2016 period. Results are depicted in Figure S3 (B, C). Our method overestimates the parks capacity factors ( 40%). One of the reasons for this could be the wake effect, as the wind is less directional in this site compared with Arauco. Although the variability is still accurate, obtaining similar values of correlation for all wind parks. Besides the bias error correlation between measured data and simulations is highly acceptable.

### Chimberas solar park

In the case of solar power generation we compared the production obtained from irradiance reanalysis data with the generation at Chimberas Solar Power Plant, a park located in San Juan with $7\,\mathrm{MW}$ of fixed tilt polycristalline silicon panels installed capacity. This information was also provided by CAMMESA. The comparison is again acceptable, as shown in Figure S3 (D). The capacity factor simulated $(0.21)$ is slightly higher than measured $(0.20)$. Correlation is very high, with an hourly value of $0.93$, probably dominated by the daily cycle. Correlating daily values gives a lower result of $0.69$. The root mean square error (RMSE) using hourly data is $48\%$ of mean power, while using daily values is $23\%$ of mean power.

Maximums of power occur during autumn and spring equinoxes, closely with summer solstices. This is because solar panels are fixed with a tilt of $28^o$, which is the value that maximizes the year round capacity factor. Moreeven, for latitudes below $30$ degrees summer solstice are the periods with least capacity if fixed panels are used. This indicates that panels fixation type strongly impacts the power time series.

## 3 OPTIMIZATION PROBLEMS

The optimization problem described in sec. **??** is formally described next. For the sake of brevity we have grouped all coefficients $a_i$ and $b_i$ into column vectors

$$\boldsymbol{a} = \left[a_1, \ldots, a_N\right]^\top \tag{S1}$$

$$\boldsymbol{b} = \left[b_1, \ldots, b_N\right]^\top \tag{S2}$$

$$\tag{S3}$$

and renamed the residual power after current installed and projected capacity as,

$$P_{\text{resid0}}(t) = P_{\text{load}}(t) - P_{\text{curr}}(t). \tag{S4}$$

We call this signal the baseline residual power, and we have that the residual power is $P_{\text{resid}}(t) = P_{\text{resid0}}(t) - P_{\text{addit}}(t)$

The objective is to minimize the variance of the residual power,

$$\operatorname{var}\left(P_{\text{resid}}\right) = \boldsymbol{b}^\top \Sigma_{w,w} \boldsymbol{b} - 2\Sigma_{P_{\text{resid0}},w} \boldsymbol{b} + \sigma^2_{P_{\text{resid0}}} \tag{S5}$$

where $\Sigma_{w,w}$ is the covariance matrix of the capacity factor signals $\left\{w_i(t)\right\}$, $\Sigma_{P_{\text{resid0}},w}$ is the covariance between the baseline residual power and the capacity factors, and the last term is the variance of the baseline residual power, i.e. residual power without additional capacity. Since this last term is not subject to optimization it can be ignored, hence the optimization problem can be stated compactly as,

**Table S2.** Installed and projected wind parks. Projected power values correspond to tenders up to RENOVAR 1.5, and are supposed to be operative in 2019. Superscript denote the origin of the project: $a$: current operational (GENREN and Resol. 108/11) $b$: RENOVAR 1, $c$: RENOVAR 1.5, $d$: RENOVAR 2, $e$ : Resol. 202/16, $f$: private initiatives. WRF values as well as all capacity factors correspond to the period from 2015-01-15 to 2016-01-14. Source: CAMMESA Online at `http://dteceolico.unrn.edu.ar/ol3/`

| ID | Province | Location | lat | lon | $\bar{v}_{h=100m}$ [m/s] MERRA | WRF | correl. MERRA-WRF | weibull $k$ MERRA | WRF | CF WRF | Power [MW] |
|---|---|---|---|---|---|---|---|---|---|---|---|
| 1 | Mendoza | San Rafael | -34.84 | -69.33 | 5.04 | 8.10 | 0.61 | 1.77 | 1.69 | 0.35 | [e]50 |
| 2 | La Rioja | Arauco | -28.75 | -66.75 | 3.98 | 7.28 | 0.36 | 2.01 | 2.16 | 0.40 | [a,b,c]272 |
| 3 | S. del Est. | El Jume | -29.42 | -63.71 | 6.56 | 9.20 | 0.66 | 3.98 | 2.94 | 0.53 | [a]8 |
| 4 | Córdoba | Achiras | -33.14 | -64.96 | 5.79 | 8.17 | 0.64 | 3.11 | 2.30 | 0.42 | [c]48 |
| 5 | Santa Fe | Rufino | -34.20 | -62.90 | 5.72 | 8.42 | 0.48 | 3.46 | 1.78 | 0.44 | [b]- |
| 6 | Bs. As. | Maipú | -37.10 | -57.80 | 7.16 | 8.09 | 0.74 | 3.29 | 2.71 | 0.44 | [b]- |
| 7 | Bs. As. | Miramar | -38.27 | -57.83 | 8.29 | 9.24 | 0.79 | 2.63 | 2.51 | 0.54 | [c]98 |
| 8 | Bs. As. | Necochea | -38.56 | -58.75 | 7.92 | 8.58 | 0.80 | 2.84 | 2.60 | 0.49 | [c]38 |
| 9 | Bs. As. | Olavarría | -36.64 | -60.34 | 6.83 | 7.86 | 0.72 | 3.09 | 2.72 | 0.46 | [d]- |
| 10 | La Pampa | Gral. Acha | -37.43 | -64.72 | 7.11 | 8.13 | 0.71 | 2.92 | 2.49 | 0.44 | [c]37 |
| 11 | Bs. As. | Tres Arroyos | -38.82 | -60.32 | 7.93 | 8.91 | 0.77 | 2.83 | 2.63 | 0.52 | [b,c]100 |
| 12 | Bs. As. | Bahía Blanca | -38.61 | -62.34 | 7.87 | 8.65 | 0.76 | 3.02 | 2.35 | 0.48 | [b,c,d]- |
| 13 | Bs. As. | Cnel. Rosales | -38.71 | -62.53 | 7.87 | 8.27 | 0.75 | 3.02 | 2.53 | 0.45 | [c]- |
| 14 | Bs. As. | Bahía Blanca | -38.36 | -62.21 | 7.87 | 8.95 | 0.76 | 3.02 | 2.46 | 0.51 | [b]10 |
| 15 | Bs. As. | Tornquist | -38.24 | -62.32 | 7.74 | 8.73 | 0.77 | 3.09 | 2.52 | 0.50 | [e]- |
| 16 | Bs. As. | Bahía Blanca | -38.62 | -62.02 | 8.11 | 8.62 | 0.78 | 3.01 | 2.62 | 0.49 | [b]100 |
| 17 | Bs. As. | Bahía Blanca | -38.67 | -61.96 | 8.11 | 8.64 | 0.77 | 3.01 | 2.65 | 0.49 | [c]- |
| 18 | Bs. As. | Villarino | -38.82 | -62.70 | 7.72 | 8.23 | 0.73 | 3.15 | 2.88 | 0.46 | [b]99 |
| 19 | Bs. As. | Buratovich | -39.25 | -62.62 | 7.82 | 8.51 | 0.71 | 3.27 | 2.89 | 0.49 | [b]50 |
| 20 | Bs. As. | Villalonga | -40.03 | -62.66 | 7.93 | 8.75 | 0.74 | 3.18 | 2.94 | 0.50 | [a,b]50 |
| 21 | Bs. As. | Carmen de Pat. | -40.55 | -63.02 | 7.87 | 8.73 | 0.73 | 3.16 | 2.72 | 0.50 | [b]- |
| 22 | Río Negro | Adolfo Alsina | -40.80 | -63.87 | 8.14 | 9.48 | 0.76 | 2.79 | 2.57 | 0.54 | [c]- |
| 23 | Río Negro | San Antonio | -40.80 | -65.20 | 7.74 | 9.05 | 0.69 | 2.48 | 2.58 | 0.53 | [b]- |
| 24 | Río Negro | Choele Choel | -39.35 | -65.59 | 7.50 | 8.12 | 0.70 | 2.88 | 2.39 | 0.44 | [c]100 |
| 25 | Chubut | Trelew | -43.12 | -65.26 | 8.58 | 9.29 | 0.73 | 2.68 | 2.38 | 0.52 | [a,b,c]248 |
| 26 | Chubut | Puerto Madryn | -42.64 | -65.26 | 8.64 | 9.09 | 0.73 | 2.78 | 2.61 | 0.54 | [f]300 |
| 27 | Chubut | Rawson | -43.35 | -65.18 | 8.47 | 9.17 | 0.77 | 2.46 | 2.61 | 0.53 | [a]101 |
| 28 | Chubut | Gastre | -42.38 | -69.28 | 8.45 | 8.70 | 0.83 | 2.58 | 2.21 | 0.48 | [b]- |
| 29 | Chubut | Garayalde | -44.71 | -66.73 | 8.97 | 9.92 | 0.77 | 2.89 | 2.58 | 0.56 | [b]24 |
| 30 | Chubut | Malaspina | -44.92 | -66.99 | 9.30 | 10.54 | 0.77 | 2.77 | 2.60 | 0.61 | [e]50 |
| 31 | Chubut | Mles. Behr | -45.67 | -67.81 | 9.88 | 11.65 | 0.81 | 2.58 | 2.50 | 0.67 | [b,d,f]100 |
| 32 | Chubut | C. Rivadavia | -45.85 | -67.50 | 9.54 | 10.93 | 0.80 | 2.35 | 1.91 | 0.58 | [a]3 |
| 33 | Chubut | C. Rivadavia | -45.78 | -67.67 | 9.54 | 12.24 | 0.80 | 2.35 | 2.09 | 0.65 | [a]6 |
| 34 | Chubut | P.del Castillo | -45.79 | -68.06 | 9.58 | 10.96 | 0.82 | 2.49 | 2.64 | 0.64 | [b]24 |
| 35 | Santa Cruz | Koluel Kaike | -46.70 | -68.40 | 9.13 | 9.87 | 0.80 | 2.52 | 2.13 | 0.56 | [e]220 |
| 36 | Santa Cruz | Las Heras | -46.55 | -68.95 | 9.05 | 10.05 | 0.83 | 2.45 | 2.21 | 0.57 | [b]97 |
| 37 | Santa Cruz | Pico Truncado | -46.82 | -67.94 | 8.62 | 10.24 | 0.75 | 2.68 | 2.41 | 0.59 | [c]- |
| 38 | Santa Cruz | Jaramillo | -47.18 | -67.14 | 8.89 | 9.77 | 0.71 | 2.76 | 2.54 | 0.56 | [c]100 |
| 39 | Santa Cruz | Puerto Deseado | -47.55 | -66.18 | 9.06 | 9.84 | 0.73 | 2.94 | 2.58 | 0.57 | [b]- |
| 40 | Santa Cruz | Piebra Buena | -49.93 | -68.85 | 9.02 | 8.77 | 0.78 | 2.56 | 2.13 | 0.48 | [c]- |
| 41 | Río Negro | Pilcaniyeu | -40.73 | -70.58 | 6.70 | 7.85 | 0.72 | 2.13 | 2.35 | 0.45 | [b]50 |
| 42 | Neuquén | Zapala | -38.86 | -70.05 | 7.24 | 7.68 | 0.75 | 2.18 | 1.72 | 0.38 | [b]- |
| 43 | Río Negro | Cerro Policía | -39.83 | -68.63 | 7.94 | 7.29 | 0.60 | 2.56 | 1.73 | 0.39 | [b]- |
| 44 | Neuquén | Senillosa | -38.93 | -68.56 | 7.05 | 7.20 | 0.72 | 2.12 | 1.76 | 0.39 | [b]- |
| 45 | Neuquén | Confluencia | -38.87 | -68.23 | 7.41 | 7.66 | 0.74 | 2.37 | 1.90 | 0.44 | [b]75 |
| 46 | Neuquén | Picún Leufú | -39.36 | -69.04 | 7.48 | 7.55 | 0.71 | 2.23 | 1.73 | 0.43 | [b]- |

$$\boldsymbol{b} = \arg\min_{\boldsymbol{x}} \frac{1}{2}\boldsymbol{x}^\top H \boldsymbol{x} + \boldsymbol{q}^\top \boldsymbol{x} \tag{S6}$$

subject to

$$\bar{\boldsymbol{w}}^\top \boldsymbol{x} = C \tag{S7}$$

$$I\boldsymbol{x} \geq \boldsymbol{x}_{\text{min}} \tag{S8}$$

**Table S3.** Solar park projects awarded in RENOVAR 1 and RENOVAR 1.5 tenders. All projects are located in the North-west region of Argentina, where the mean irradiances above 200 W/m$^2$, over 300 W/m$^2$ in two cases. Chimberas (fixed panels) and San Juan 1 (Gambetta and Doña, 2011) (fixed, 1D and 2D tracking panels) are already operational projects. The rest of the projects have 1D tracking panels except Caucharí with fixed panels. Source: CAMMESA.

| ID | Name | Province | lat | lon | $\bar{Irr}$ [W/m$^2$] | CF | Power [MW] |
|---|---|---|---|---|---|---|---|
| 47 | Lavalle | MENDOZA | -32.71 | -68.52 | 249 | 0.25 | 17.60 |
| 48 | Lujan de Cuyo | MENDOZA | -33.07 | -69.05 | 244 | 0.24 | 22.00 |
| 49 | La Paz | MENDOZA | -33.48 | -67.56 | 238 | 0.23 | 14.08 |
| 50 | PASIP | MENDOZA | -33.04 | -68.54 | 244 | 0.24 | 1.15 |
| 51 | General Alvear | MENDOZA | -35.04 | -67.66 | 232 | 0.23 | 17.60 |
| 52 | Cafayate | SALTA | -26.03 | -65.94 | 284 | 0.32 | 80.00 |
| 53 | Nonogasta | LA RIOJA | -29.33 | -67.42 | 262 | 0.27 | 35.00 |
| 54 | Fiambalá | CATAMARCA | -27.74 | -67.64 | 283 | 0.31 | 11.00 |
| 55 | Tinogasta | CATAMARCA | -28.04 | -67.54 | 268 | 0.28 | 15.00 |
| 56 | Saujil | CATAMARCA | -28.16 | -66.22 | 264 | 0.27 | 22.50 |
| 57 | Sarmiento | SAN JUAN | -31.97 | -68.48 | 254 | 0.26 | 35.00 |
| 58 | Ullum | SAN JUAN | -33.31 | -68.89 | 259 | 0.26 | 95.50 |
| 59 | Anchoris | MENDOZA | -33.30 | -66.39 | 242 | 0.24 | 21.30 |
| 60 | Caldenes del Oeste | SAN LUIS | -33.32 | -66.17 | 234 | 0.24 | 24.75 |
| 61 | La cumbre | SAN LUIS | -31.30 | -68.67 | 234 | 0.24 | 22.00 |
| 62 | Iglesia- Guañizuli | SAN JUAN | -30.34 | -69.27 | 280 | 0.31 | 80.00 |
| 63 | Las Lomitas | SAN JUAN | -30.59 | -67.52 | 255 | 0.26 | 1.70 |
| 64 | La Puna | SALTA | -24.27 | -66.20 | 304 | 0.35 | 100.00 |
| 65 | Cauchari | JUJUY | -24.10 | -66.73 | 313 | 0.27 | 300.00 |
| 66 | Chimberas | SAN JUAN | -31.99 | -68.54 | 246 | 0.20 | 7 |
| 67 | San Juan 1 | SAN JUAN | -31.39 | -68.68 | 246 | 0.22 | 1.2 |

by defining $H = 2\Sigma_{w,w} \in \mathbb{R}^{N\times N}$ and $\boldsymbol{q}^\top = -2\Sigma_{P_{\text{resid0}},w} \in \mathbb{R}^{1\times N}$. The vector $\bar{\boldsymbol{w}}$ is a $N$-column vector filled with the mean values of the site's capacity factors. This constraint implements the constraint in equation (S7). This problem can be solved by quadratic programming (QP) using a null-space active-set method.

Another interesting optimization problem is the one of minimizing the variance to square mean ratio. The mean of the residual power is,

$$\overline{P_{\text{resid}}} = \overline{P_{\text{resid0}}} - \boldsymbol{b}^\top \bar{\boldsymbol{w}} \tag{S9}$$

The minimization problem reads,

$$\boldsymbol{b} = \arg\min_{\boldsymbol{x}} \frac{\boldsymbol{x}^\top \Sigma_{w,w}\boldsymbol{x} - 2\Sigma_{P_{\text{resid0}},w}\boldsymbol{x} + \sigma^2_{P_{\text{resid0}}}}{\left(\overline{P_{\text{resid0}}} - \boldsymbol{x}^\top \bar{\boldsymbol{w}}\right)^2} \tag{S10}$$

subject to

$$\bar{\boldsymbol{w}}^\top \boldsymbol{x} = C \tag{S11}$$

$$I\boldsymbol{x} \geq \boldsymbol{x}_{\min} \tag{S12}$$

This problem is not quadratic anymore, and is equivalent to the one with the logarithm of the cost function, i.e.

$$
\begin{aligned}
\boldsymbol{b} = \arg\min_{\boldsymbol{x}} \log\Big(&\boldsymbol{x}^\top \Sigma_{w,w}\boldsymbol{x} - 2\Sigma_{P_{\text{resid0}},w}\boldsymbol{x}+\\
&\sigma^2_{P_{\text{resid0}}}\Big) - 2\log\left(\overline{P_{\text{resid0}}} - \boldsymbol{x}^\top\bar{\boldsymbol{w}}\right) \qquad \text{(S13)}\\
&\text{subject to}\\
&\quad \bar{\boldsymbol{w}}^\top\boldsymbol{x} = C \qquad \text{(S14)}\\
&\qquad I\boldsymbol{x} \geq \boldsymbol{x}_{\min} \qquad \text{(S15)}
\end{aligned}
$$

which is suitable, for example, for sequential quadratic programming.

## REFERENCES


Commission, I. E. et al. (2005). International standard iec 61400-1. *Wind turbine generator systems-part* 1

Gambetta, P. and Doña, V. M. (2011). Planta solar fotovoltaica san juan 1: Descripción de se diseño y detalles de operación. *Cuarto Congreso Nacional – Tercer Congreso Iberoamericano Hidrógeno y Fuentes Sustentables de Energía – HYFUSEN 2011*

Pfenninger, S. and Staffell, I. (2016). Long-term patterns of european pv output using 30 years of validated hourly reanalysis and satellite data. *Energy* 114, 1251–1265

Rhodes, B. C. (2011). Pyephem: astronomical ephemeris for python. *Astrophysics Source Code Library*

Ridley, B., Boland, J., and Lauret, P. (2010). Modelling of diffuse solar fraction with multiple predictors. *Renewable Energy* 35, 478–483

Staffell, I. and Green, R. (2014). How does wind farm performance decline with age? *Renewable energy* 66, 775–786

Staffell, I. and Pfenninger, S. (2016). Using bias-corrected reanalysis to simulate current and future wind power output. *Energy* 114, 1224–1239